LETTER

Structure and dynamics of a glass-forming binary complex plasma with non-reciprocal interaction

To cite this article: Yi-Fei Lin *et al* 2018 *EPL* **123** 35001

A Letters Journal Exploring the Frontiers of Physics

August 2018

EPL, **123** (2018) 35001 www.epljournal.org
doi: 10.1209/0295-5075/123/35001

Structure and dynamics of a glass-forming binary complex plasma with non-reciprocal interaction

Yi-Fei Lin[1], Alexei Ivlev[2], Hartmut Löwen[3], Liang Hong[4] and Cheng-Ran Du[1,5(a)]

[1] *College of Science, Donghua University - 201620 Shanghai, PRC*
[2] *Max Planck Institute for Extraterrestrial Physics - 85748 Garching, Germany*
[3] *Institut für Theoretische Physik II: Weiche Materie, Heinrich-Heine-Universität Düsseldorf 40225 Düsseldorf, Germany*
[4] *School of Physics and Astronomy & Institute of Natural Sciences, Shanghai Jiao Tong University 200240 Shanghai, PRC*
[5] *Member of Magnetic Confinement Fusion Research Centre, Ministry of Education - PRC*

received 16 May 2018; accepted in final form 14 August 2018
published online 10 September 2018

PACS 52.27.Lw – Dusty or complex plasmas; plasma crystals

Abstract – In this letter, a simulation study on the structural and dynamical properties of a quasi-two-dimensional (q2D) binary complex plasma with Langevin dynamics is presented. The effect of a non-reciprocal interaction on the structure is investigated by comparing systems with pure Yukawa and with point-wake Yukawa interactions. The long-time alpha-relaxation for the latter system is revealed by plotting and analyzing the intermediate scattering function. The results clearly indicate that a q2D binary complex plasma is a suitable model system to study the dynamics of a glass former. The non-reciprocity of the interactions shifts the glass formation significantly but leads to the same qualitative signatures as in the reciprocal case.

Introduction. – A complex plasma consists of micron-sized particles immersed in a low-temperature plasma [1]. The particles interact with ions and electrons and acquire high charges Q. Since the thermal velocity of electrons is much higher than that of ions, the charges Q usually are negative. The particles interact with each other via a screened Coulomb interaction. The interplay between the damping (caused by a neutral gas) and the heating mechanism (such as charge fluctuation) results in a finite kinetic temperature T. In a complex plasma, the microparticles are the dominant species in terms of the energy and momentum transport and, therefore, the system can be viewed as an effective one-component material. Furthermore, complex plasmas represent an open non-Hamiltonian system and can exist in gaseous, liquid and solid phases [2,3]. Therefore, they are ideal model systems to study classical condensed matter at the "atom" (*i.e.*, particle resolved) level [4,5].

Since the discovery of plasma crystals [6,7], complex plasmas have been used to study the dynamics of various phenomena such as melting [8,9], recrystallzation [10], defect transport [11], formation of Mach cones [12,13], etc. Particularly in laboratory experiments, the particles are suspended in the sheath area above the bottom electrode and form a layer of particles. These charged particles divert the ion flow in the sheath, leading to a focus of positive charged ions beneath the microparticles, known as ion wake effect. The presence of high ion densities exerts an additional force on the neighboring microparticles. For a binary mixture of microparticles levitating at a slightly different height above the electrode, the effect of this additional force is uneven, resulting in non-reciprocal effective interactions between the particles [14]. Of course, this does not violate the principles of Newton's action = reaction, since the flowing ions are carrying momentum away (one should keep in mind that the ion wakes are not attached to the charged particles, but are induced in the surrounding flowing plasma). Therefore, the momentum of the microparticles is no longer conserved. We point out that the interaction non-reciprocity has not only been previously used [4,5,15–22] and experimentally tested in complex plasmas [13,14,23–29], but it has been also observed in many other systems [30–39].

As a liquid is cooled, it may not only crystallize but also remain in an amorphous state [40,41]. A supercooled liquid can exhibit glassy dynamics. Recently, a glass

(a) E-mail: chengran.du@dhu.edu.cn

former was discovered experimentally in a quasi-two-dimensional (q2D) binary complex plasma [42]. With a dilute background gas, the system can be seen as virtually undamped [4]. Unlike colloidal glasses which obey overdamped dynamics, this enables one to study a glass former which is governed by the same equations of motion as molecular glasses albeit on a much larger length scale [18,42].

In this letter, we report on a Langevin dynamics simulation of a q2D binary complex plasma. We study the dependence of the structure on the number ratio of two particle types and focus on the dynamics of the long time scale, namely the alpha-relaxation. Fitting the self-part of the intermediate scattering function using a Kohlrausch equation, we determine the critical parameters for the glass transition of the system.

The implications of this study are twofold: first we show that in an appropriate model for a binary complex plasma a glass transition does occur. Hence complex plasmas can be used to explore the slowing-down in the dynamics. Second, on a more fundamental level, the effect of non-reciprocal interactions on the glass transition has not yet been studied. Computer simulation so far assumed reciprocal interactions and mode coupling theory typically requires Hamiltonian systems with reciprocal interactions. Our study reveals that non-reciprocal interactions shift the glass transition relative to that in reciprocal systems but the qualitative scenario and signatures are the same.

Simulation. – In complex plasmas, the motions of microparticles can be studied by molecular dynamics (MD). The equations of motion including damping read

$$m_i\ddot{\boldsymbol{r}}_i + m_i\nu\dot{\boldsymbol{r}}_i = \sum_j \boldsymbol{F}_{ji} + \boldsymbol{L}_i, \tag{1}$$

where $\boldsymbol{r}_i$ is the particle position, m_i the mass, ν_i the damping rate, $\boldsymbol{L}_i$ the Langevin heat bath. The Langevin force $\boldsymbol{L}_i$ is defined by $\langle \boldsymbol{L}_i(t)\rangle = 0$ and $\langle \boldsymbol{L}_i(t)\boldsymbol{L}_i(t+\tau')\rangle = 2\nu_i m_i T\delta(\tau')\mathbf{I}$, where t is the time, T is the temperature of the heat bath, $\delta(\tau')$ is the delta function and $\mathbf{I}$ is the unit matrix.

Here we simulated a binary mixtures of microparticles confined in the (pre)sheath of a plasma, where the gravitational force is balanced by the electrostatic forces of the sheath field [42–44]. Since two types of particle have different mass, the equilibrium heights deviate. Generally, this vertical strong confinement can be modeled using parabolic confinement. However, recent experiments show that under certain conditions, the vertical motion is much smaller compared with the horizontal one [42]. Therefore, for simplicity we neglected the vertical motion and considered the height difference as a constant Δ, see fig. 1. Experiments show that Δ depends on the disparity of two types of particles, gas pressure and discharge power, but does not depend on the interparticle distance.

In the simulation, individual microparticles are modeled as negative point-like charges. To include the ion wake

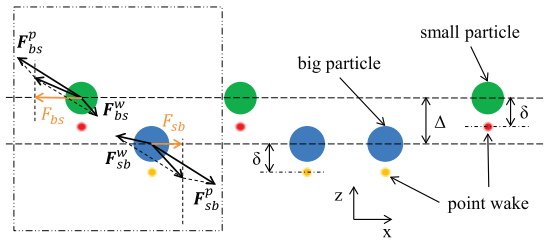

Fig. 1: (Color online) A sketch showing the side view of a quasi-two-dimensional complex plasma. The non-reciprocal interaction between a small particle and a big particle is illustrated.

in the particle interaction, a positive point-like charge is placed at a fixed vertical distance δ below each particle [19–22,25,27–29]. The force exerted on particle i by particle j is composed of two components, namely the repulsive force $\boldsymbol{F}^p_{ji}$ by particle j and attractive force $\boldsymbol{F}^w_{ji}$ by the point-like charge below particle j. Both components have the form of a Yukawa interaction, see fig. 1. The effective forces can be written as

$$\boldsymbol{F}_{ji} = \boldsymbol{F}^p_{ji} + \boldsymbol{F}^w_{ji} = Q_iQ_jf(r_{ji})\frac{\boldsymbol{r}_{ji}}{r_{ji}} + q_iQ_jf(r^w_{ji})\frac{\boldsymbol{r}^w_{ji}}{r^w_{ji}}, \tag{2}$$

where $f(r) = \exp(-r/\lambda)(1+r/\lambda)/4\pi\epsilon_0 r^2$, λ is the effective screening length, $\boldsymbol{r}_{ji} = \boldsymbol{r}_i - \boldsymbol{r}_j$ and $\boldsymbol{r}^w_{ji} = \boldsymbol{r}_i - (\boldsymbol{r}_j - \delta\boldsymbol{e}_z)$. Without the vertical motion, we projected forces in the xy plane and the system becomes essentially 2D. Thus, the interaction is non-reciprocal [14,17,26]. The molecular-dynamics simulations were performed using LAMMPS in the canonical ensemble [45,46].

We choose typical plasma and particle parameters according to the experiments [42]. The neutral gas pressure is 0.65 Pa (which determines the damping). The small particles have a diameter $d_s = 9.19\,\mu$m, and a mass $m_s = 6.13\times10^{-13}$ kg. The big particles have a diameter $d_b = 11.36\,\mu$m, and a mass $m_b = 8.03\times10^{-13}$ kg. The charge are set to $Q_s = 7280\ e$ and $Q_b = 11200\ e$ and the screening length is $\lambda = 400\,\mu$m, deduced from the measurement of phonon spectra in plasma crystals of these two types of particles separately in experiments [47]. The damping rates are calculated based on the Epstein formalism $\nu_\alpha \propto \gamma_{Ep}d_\alpha^2$ ($\alpha = b, s$), where we select $\gamma_{Ep} = 1.26$ [48–50]. The rates are set to $\nu_s = 0.77\,\mathrm{s}^{-1}$ and $\nu_b = 0.91\,\mathrm{s}^{-1}$ for small and big particles, respectively. The small particles are levitated by 160 μm higher than the big particles, according to the direct measurement in the experiments [42]. For the point-wake model, we fix the vertical distance of the point wake to the particle as 40 μm and the point-wake charge is 20% of the particle charge [27].

The resulting interaction in the horizontal direction with the point-wake model is shown in fig. 2(a). As we can see in the figure, the interaction between the same type of particles is always repulsive. Due to the higher charge, the repulsive force between big particles F_{bb} is larger than that between small particles F_{ss}. However, the force acting on a small particle by a big particle and its wake (F_{bs})

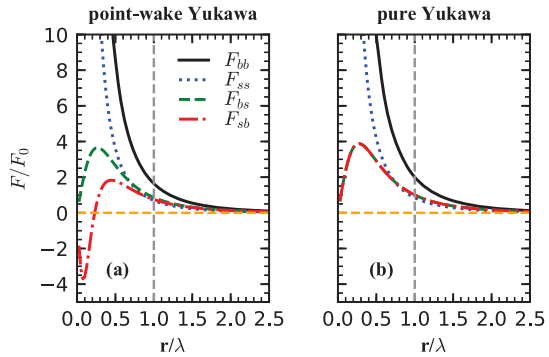

Fig. 2: (Color online) The force F between two particles with (a) and without (b) considering the wake effect. The force is normalized to a characteristic value of $F_0 = Q_s Q_b/4\pi\epsilon_0\lambda^2$. A positive value means repulsive and a negative value means attractive. The yellow horizontal dashed line marks the zero force and the grey vertical dashed line highlights the screening length. Because the small and big particles are in different layers, the forces in the pure Yukawa case are non-monotonic.

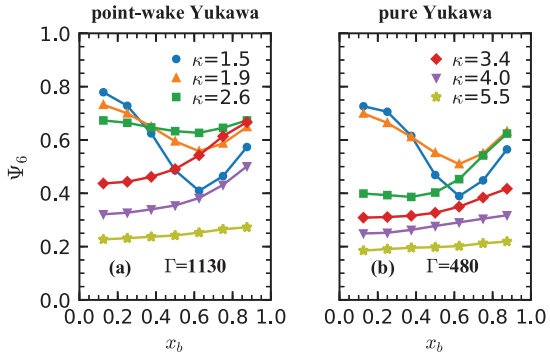

Fig. 3: (Color online) Dependence of averaged hexatic order parameter Ψ_6 on the number ratio of big particles x_b with (a) and without (b) considering the wake effect. For the point-wake model and Yukawa interaction, the selected Γ is 1130 and 480, respectively.

is larger than the force on a big particle by a small particle and its wake (F_{sb}). Moreover, at very small distance, the later shows an attractive force due to the presence of the wake. In the point-wake model, the interaction is indeed non-reciprocal. For comparison, we show the interaction without considering the wake effect (only the F^p_{ji} term in eq. (2)) in fig. 2(b). The interaction is then reciprocal.

We select the kinetic temperature T and interparticle distance a as control parameters. The temperature is determined by measuring the velocities of individual particles in the xy plane, while the interparticle distance is determined from the first peak in the pair correlation function. We normalize the interparticle distance a to the screening length, thus introducing the dimensionless screening parameter:

$$\kappa = \frac{a}{\lambda}. \tag{3}$$

Furthermore, we normalize the temperature T by the characteristic interaction potential of the big and small particles at a distance λ, thus introducing an effective coupling parameter Γ for a binary system:

$$\Gamma = \frac{Q_b Q_s}{4\pi\epsilon_0\lambda kT}. \tag{4}$$

Time is normalized to the damping rate of small particle ν_s. To mitigate the influence of the initial condition, we fix the spatial distribution of particles scaled to the desired interparticle distance. For each pair of control parameters, at least four different initial distributions are probed. It turns out that the initial condition has marginal influence on the relaxation and structural properties.

Results. – For a one-component complex plasma, particles form a plasma crystal at a certain temperature as κ decreases below a critical value. In binary mixtures crystallization is prevented. The local structure of a complex plasma can be characterized by a time average of a local transient hexatic order parameter ψ^i_6,

$$\bar{\psi}^i_6 = \frac{1}{\tau_a}\int_{t'}^{t'+\tau_a} \mathrm{d}t|\psi^i_6| \quad \text{and} \quad \psi^i_6 = \frac{1}{n_i}\sum_m e^{j6\theta^i_m}, \tag{5}$$

where n_i is the number of nearest neighbors of particle i and θ^i_m is the angle between $\mathbf{r}_m - \mathbf{r}_i$ and the x-axis projected in the xy plane. We select $\tau_a = 10\,\mathrm{s}$ for the average. For a system composed of many particles, we average ψ^i_6 over all the particles included in the system and obtain a structure parameter $\Psi_6 = \sum_i \bar{\psi}^i_6/N$, where N is the number of particles. Here $\Psi_6 = 1$ means a perfectly ordered crystal with hexagonal structure, while $\Psi_6 = 0$ means random arrangement.

In fig. 3(a), we plot Ψ_6 *vs.* composition of two particle species $x_b = n_b/(n_s + n_b)$ at $\Gamma = 1130$. For big κ ($\kappa > 4.0$), Ψ_6 increases as the percentage of big particles increases. This slow increase is caused by the increase of the coupling parameters since the big particles have more charges. However, for all these κ and x_b, Ψ_6 is below 0.6. The structure is quasi-random. As κ further decreases to 3.4, a crystal structure emerges as the coupling increases. For $\kappa = 2.6$, the system shows an ordered structure. For $\kappa = 1.9$, 1.5, the system exhibits ordered structure as either species dominates regardless of the coupling strength. However, for the two types of particles with similar portions, the crystalline order is suppressed. The minimum of Ψ_6 is close to $x_b \approx 0.6$. For simplicity, we use a binary mixture with $x_b = 0.5$ for the study in the sequel.

For comparison, we test the dependence of the order parameter on the composition without considering the wake effect. At $\Gamma = 1130$, the system has an ordered structure regardless of the ratio for all the selected κ. A similar trend emerges if we increase the kinetic temperature so that $\Gamma = 480$, as we show in fig. 3(b). For small κ, the crystal structure is suppressed as $x_b \approx 0.6$.

We show the spatial distribution of ψ_6 at different κ in fig. 4. As one can see, at $\Gamma = 1130$ small and big particles

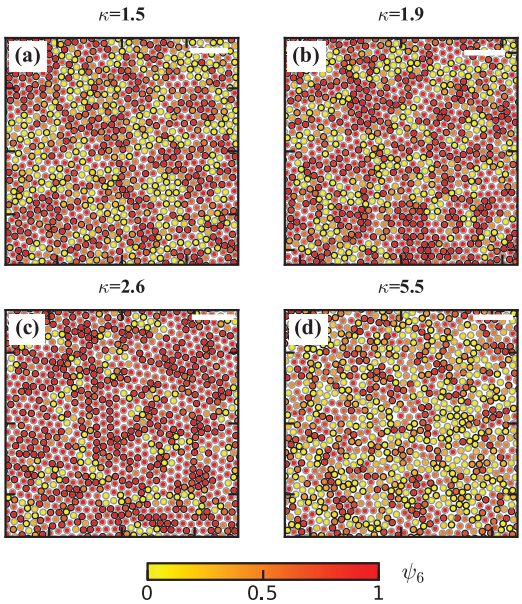

Fig. 4: (Color online) Snapshots of particle positions in the q2D binary complex plasma with point-wake Yukawa interaction at $\Gamma = 1130$. Big particles have a black outlines while the small particles have a grey outlines. The filled color coded from yellow to red shows the Ψ_6 from 0 to 1 The white bar shows ten inter-particle distances.

are homogeneously distributed in the area. For small κ, the local structure of most particles is random though one can see clusters of hexagonal structure (yellow blobs). The size of the such cluster increases as κ increases until the majority particle are arranged in a hexagonal structure. However, as the coupling further decreases, particles start to arrange randomly again, as shown in fig. 4(d). This trend agrees with fig. 3(a) for $x_b = 0.5$.

We plot the averaged hexatic order parameter Ψ_6 in the (Γ, κ)-space to gain a general picture, as shown in fig. 5(a). As the system cools down, the fast motion of particles decreases and the order starts to build up. As we can see in the figure, the lower the temperature is, the more ordered the particles are. For small κ, the structure does not change much for low temperature but hexagonal order builds up as temperature decreases in the "hot" regime. For big κ, temperature of this fast changing regime is substantially lower. Note that for a certain temperature, the change of the structure is not monotonic against κ. There is only a window of κ in which the system forms a hexagonal ordered structure.

Again we plot Ψ_6 in the (Γ, κ)-space for a Yukawa system without considering the wake in fig. 5(b). For the same pair of Γ and κ, Ψ_6 has a higher value, representing ordered structure. This is caused by the higher coupling if the wake is absent. However, the hexagonal structure is formed in a larger parameter window in the diagram. This shows that for the reciprocal and non-reciprocal system, the formation of ordered structure has a qualitatively similar trend in the parameter range of interest in a binary complex plasma.

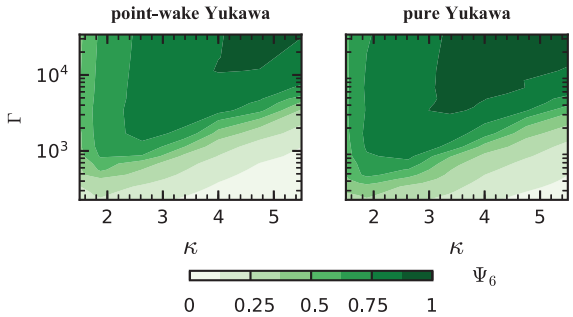

Fig. 5: (Color online) The averaged hexatic order parameter Ψ_6 in the (Γ, κ)-plane, for a binary complex plasma with (a) and without (b) considering the wake effect.

The structural relaxation is generally quantified by the density-density correlation function in $\mathbf{q}$-space, $F(q,t)$, which is the Fourier-transformation of the van Hove correlation function [51], commonly referred to as the intermediate scattering function (ISF). For practical purposes, it is convenient to use the self-part of ISF to describe the evolution of single-particle correlations

$$\mathcal{F}_(q,t) = N^{-1}\left\langle \sum_i^N \exp\{-i\mathbf{q}\cdot[\mathbf{r}_i(t+t_0)-\mathbf{r}_i(t_0)]\}\right\rangle, \tag{6}$$

where $\mathbf{r}_i(t)$ is the position of the particle i at the moment t, and $\langle\ldots\rangle$ denotes the canonical average (over t_0). $\mathbf{q}$ is the wave number and we select $|\mathbf{q}| = \pi/a$ [52–57]. As a glass former, the system keeps evolving due to effects such as aging, which is beyond the scope of this paper. In this paper, we focus on structural relaxation of the system in the slow transient state. Nevertheless, for the time frame of 100 s, there is no observable time dependence of the ISF and thus we average the $\mathcal{F}$ within this time frame to obtain a smooth relaxation curve.

A stretched-exponential (Kohlrausch) law [51,53,58–61],

$$\mathcal{F}(q,t) \simeq A(q)\exp\{-[t/\tau(q)]^{\beta(q)}\}, \tag{7}$$

usually provides a good fit for the long-time asymptotics of the ISF, the so-called alpha-relaxation. The law is determined by three parameters: the amplitude factor $A(q)$, the timescale of the alpha-relaxation $\tau(q)$ (which is also normalized to the damping rate ν_s), and the stretching exponent $\beta(q) < 1$. Selecting a time domain appropriate for the fit is generally not an easy task [53,59,62,63] – an overlap with the transient beta-relaxation should be avoided, which imposes the lower time limit for the fit.

In fig. 6(a) we plot the ISF of a system with wake-point Yukawa interaction for different Γ ranging from 340 to 3400 at $\kappa = 2.6$. For $\Gamma = 3400$, $\mathcal{F}$ shows a small drop at $t\nu_s \approx 0.6$, representing the beta-relaxation. It then reaches a plateau without significant drop within the time of numerical experiment. As temperature increases,

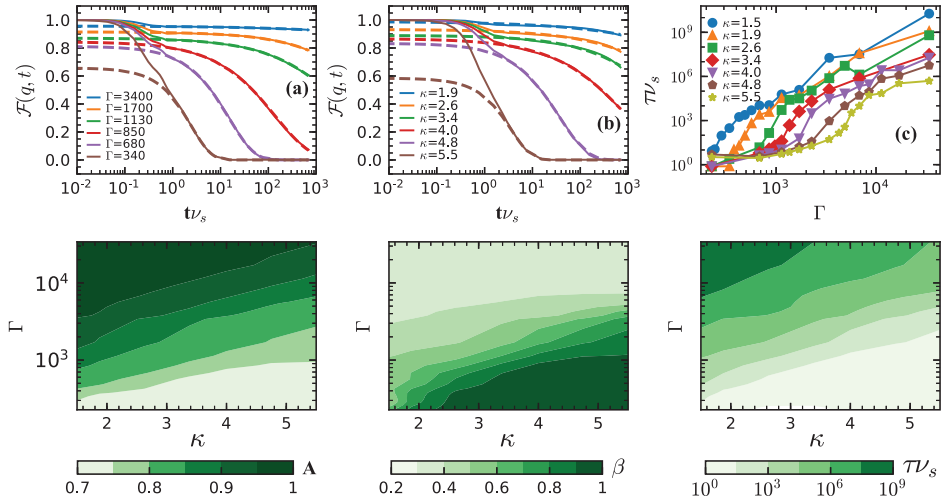

Fig. 6: (Color online) Intermediate scattering function (ISF) for varying temperature at $\kappa = 2.6$ (a) and for varying κ at $\Gamma = 1700$ (b) in a q2D binary complex plasma. The wave number q is set equal to π/a. For selected κ, the relation between the fitted τ and Γ is plotted in (c). The ISFs are fitted by Kohlrausch law, the lower panel shows the fitting parameter A (d), β (e), and τ (f) in the (Γ, κ) plane.

one can see clearly the long-time alpha-relaxation, separated by the plateau from the beta-relaxation. For very high temperature ($\Gamma = 340$), the plateau disappears and two steps of relaxation start to merge. To complement fig. 6(a), we fix a kinetic temperature ($\Gamma = 1700$) and plot the ISFs for various κ in fig. 6(b). Similarly, we see the plateau between alpha- and beta-relaxation for small κ, which vanishes for big κ.

It is instructive to look into the relation between $\tau\nu_s$ and Γ. As we see in fig. 6(c), for all κ, $\tau\nu_s$ first increases slowly with Γ and the increase becomes steep. For small temperature, this increase becomes slow again.

The Kohlrausch amplitude A, the characteristic relaxation time τ, and the stretching exponents β are plotted in the (Γ, κ)-space in fig. 6(d)–(f), respectively. As we can see, the relaxation time decreases dramatically with interpaticle distance and kinetic temperature. A decreases from 1 to 0.7 as κ increases from 2 to 5 and Γ decreases from 30000 to 300. The stretching exponents show a similar trend.

Conclusion. – Using computer simulations we have explored the glass transition in a binary model appropriate for a binary dusty plasma sheet with non-reciprocal interactions induced by the presence of a wake charge. As a reference, we have computed also the corresponding behavior of a Yukawa system without wake charge with reciprocal interactions. Non-reciprocal interactions shift the location where the dynamics is slowing down significantly but do not change the qualitative signature of the glass transition. This is interesting as *a priori* one could have expected that the local heating induced by non-reciprocity had led to a different dynamical crossover. For the future it would be interesting to establish a connection between our kind of non-reciprocity and that occurring in active systems where jamming and vitrification has also been recently found [64–68].

* * *

The authors acknowledge support from the National Natural Science Foundation of China (NSFC), Grant Nos. 11405030, 11504231, and 31630002. We are thankful for the support to this work by the Deutsche Forschungsgemeinschaft (DFG) through the grants IV 20/3-1 (for AI) and LO 418/23-1 (for HL).

REFERENCES

[1] Fortov V., Ivlev A., Khrapak S., Khrapak A. and Morfill G., *Phys. Rep.*, **421** (2005) 1.
[2] Hamaguchi S., Farouki R. T. and Dubin D. H. E., *Phys. Rev. E*, **56** (1997) 4671.
[3] Hartmann P., Kalman G. J., Donkó Z. and Kutasi K., *Phys. Rev. E*, **72** (2005) 026409.
[4] Morfill G. E. and Ivlev A. V., *Rev. Mod. Phys.*, **81** (2009) 1353.
[5] Chaudhuri M., Ivlev A. V., Khrapak S. A., Thomas H. M. and Morfill G. E., *Soft Matter*, **7** (2011) 1287.
[6] Thomas H. M. and Morfill G. E., *Nature*, **379** (1996) 806.
[7] Chu J. H. and I L., *Phys. Rev. Lett.*, **72** (1994) 4009.
[8] Rubin-Zuzic M., Morfill G. E., Ivlev A. V., Pompl R., Klumov B. A., Bunk W., Thomas H. M., Rothermel H., Havnes O. and Fouquet A., *Nat. Phys.*, **2** (2006) 181.
[9] Nosenko V., Zhdanov S. K., Ivlev A. V., Knapek C. A. and Morfill G. E., *Phys. Rev. Lett.*, **103** (2009) 015001.
[10] Knapek C. A., Samsonov D., Zhdanov S., Konopka U. and Morfill G. E., *Phys. Rev. Lett.*, **98** (2007) 015004.

[11] Nosenko V., Zhdanov S. and Morfill G., *Phys. Rev. Lett.*, **99** (2007) 025002.
[12] Samsonov D., Goree J., Thomas H. M. and Morfill G. E., *Phys. Rev. E*, **61** (2000) 5557.
[13] Du C.-R., Nosenko V., Zhdanov S., Thomas H. M. and Morfill G. E., *EPL*, **99** (2012) 55001.
[14] Ivlev A. V., Bartnick J., Heinen M., Du C.-R., Nosenko V. and Löwen H., *Phys. Rev. X*, **5** (2015) 011035.
[15] Tsytovich V. N., *Phys. Usp.*, **40** (1997) 53.
[16] Khrapak S. A., Ivlev A. V. and Morfill G., *Phys. Rev. E*, **64** (2001) 046403.
[17] Schweigert V. A., Schweigert I. V., Melzer A., Homann A. and Piel A., *Phys. Rev. E*, **54** (1996) 4155.
[18] Ivlev A., Löwen H., Morfill G. and Royall C. P., *Complex Plasmas and Colloidal Dispersions: Particle-Resolved Studies of Classical Liquids and Solids* (World Scientific, Singapore) 2012.
[19] Röcker T. B., Ivlev A. V., Kompaneets R. and Morfill G. E., *Phys. Plasmas*, **19** (2012) 033708.
[20] Zhdanov S. K., Ivlev A. V. and Morfill G. E., *Phys. Plasmas*, **16** (2009) 083706.
[21] Yazdi A., Heinen M., Ivlev A., Löwen H. and Sperl M., *Phys. Rev. E*, **91** (2015) 052301.
[22] Ivlev A. V. and Morfill G., *Phys. Rev. E*, **63** (2000) 016409.
[23] Liu B., Goree J. and Feng Y., *Phys. Rev. Lett.*, **105** (2010) 085004.
[24] Couëdel L., Nosenko V., Ivlev A. V., Zhdanov S. K., Thomas H. M. and Morfill G. E., *Phys. Rev. Lett.*, **104** (2010) 195001.
[25] Steinberg V., Sütterlin R., Ivlev A. V. and Morfill G., *Phys. Rev. Lett.*, **86** (2001) 4540.
[26] Melzer A., Schweigert V. A. and Piel A., *Phys. Rev. Lett.*, **83** (1999) 3194.
[27] Laut I., Räth C., Zhdanov S. K., Nosenko V., Morfill G. E. and Thomas H. M., *Phys. Rev. Lett.*, **118** (2017) 075002.
[28] Couëdel L., Zhdanov S., Nosenko V., Ivlev A. V., Thomas H. M. and Morfill G. E., *Phys. Rev. E*, **89** (2014) 053108.
[29] Laut I., Zhdanov S. K., Räth C., Thomas H. M. and Morfill G. E., *Phys. Rev. E*, **93** (2016) 013204.
[30] Hayashi K. and ichi Sasa S., *J. Phys.: Condens. Matter*, **18** (2006) 2825.
[31] Buenzli P. R. and Soto R., *Phys. Rev. E*, **78** (2008) 020102.
[32] Shanblatt E. R. and Grier D. G., *Opt. Express*, **19** (2011) 5833.
[33] Dholakia K. and Zemánek P., *Rev. Mod. Phys.*, **82** (2010) 1767.
[34] Sabass B. and Seifert U., *Phys. Rev. Lett.*, **105** (2010) 218103.
[35] Soto R. and Golestanian R., *Phys. Rev. Lett.*, **112** (2014) 068301.
[36] Dzubiella J., Löwen H. and Likos C. N., *Phys. Rev. Lett.*, **91** (2003) 248301.
[37] Mejia-Monasterio C. and Oshanin G., *Soft Matter*, **7** (2011) 993.
[38] Sriram I. and Furst E. M., *Soft Matter*, **8** (2012) 3335.
[39] Khair A. S. and Brady J. F., *Proc. R. Soc. London, Ser. A: Math. Phys. Eng. Sci.*, **463** (2007) 223.
[40] Debenedetti P. G. and Stillinger F. H., *Nature*, **410** (2001) 259.
[41] Berthier L. and Biroli G., *Rev. Mod. Phys.*, **83** (2011) 587.
[42] Du C.-R., Nosenko V., Thomas H. M., Morfill G. E. and Ivlev A. V., arXiv: 1609.01456 (2016).
[43] Hartmann P., Donkó Z., Kalman G. J., Kyrkos S., Golden K. I. and Rosenberg M., *Phys. Rev. Lett.*, **103** (2009) 245002.
[44] Wieben F., Schablinski J. and Block D., *Phys. Plasmas*, **24** (2017) 033707.
[45] *Lammps molecular dynamics simulator*, `http://lammps.sandia.gov`.
[46] Plimpton S., *J. Comput. Phys.*, **117** (1995) 1.
[47] Nunomura S., Goree J., Hu S., Wang X. and Bhattacharjee A., *Phys. Rev. E*, **65** (2002) 066402.
[48] Epstein P. S., *Phys. Rev.*, **23** (1924) 710.
[49] Liu B., Goree J., Nosenko V. and Boufendi L., *Phys. Plasmas*, **10** (2003) 9.
[50] Konopka U., Morfill G. E. and Ratke L., *Phys. Rev. Lett.*, **84** (2000) 891.
[51] Hansen J. and McDonald I., *Theory of Simple Liquids* (Elsevier Science) 2006.
[52] Fuchs M., Götze W. and Mayr M. R., *Phys. Rev. E*, **58** (1998) 3384.
[53] Voigtmann T., Puertas A. M. and Fuchs M., *Phys. Rev. E*, **70** (2004) 061506.
[54] Bayer M., Brader J. M., Ebert F., Fuchs M., Lange E., Maret G., Schilling R., Sperl M. and Wittmer J. P., *Phys. Rev. E*, **76** (2007) 011508.
[55] Flenner E. and Szamel G., *Nat. Commun.*, **6** (2015) 7392.
[56] Kawasaki T., Araki T. and Tanaka H., *Phys. Rev. Lett.*, **99** (2007) 215701.
[57] Vivek S., Kelleher C. P., Chaikin P. M. and Weeks E. R., *Proc. Natl. Acad. Sci. U.S.A.*, **114** (2017) 1850.
[58] Franosch T., Fuchs M., Götze W., Mayr M. R. and Singh A. P., *Phys. Rev. E*, **55** (1997) 7153.
[59] Fuchs M., Hofacker I. and Latz A., *Phys. Rev. A*, **45** (1992) 898.
[60] Fuchs M., *J. Non-Crystal. Solids*, **172** (1994) 241.
[61] Feng Y., Goree J. and Liu B., *Phys. Rev. E*, **82** (2010) 036403.
[62] Bartsch E., Antonietti M., Schupp W. and Sillescu H., *J. Chem. Phys.*, **97** (1992) 3950.
[63] Phillips J. C., *Rep. Prog. Phys.*, **59** (1996) 1133.
[64] Flenner E., Szamel G. and Berthier L., *Soft Matter*, **12** (2016) 7136.
[65] Berthier L., Flenner E. and Szamel G., *New J. Phys.*, **19** (2017) 125006.
[66] Nandi S. K. and Gov N. S., *Soft Matter*, **13** (2017) 7609.
[67] Janssen L. M. C., Kaiser A. and Löwen H., *Sci. Rep.*, **7** (2017) 5667.
[68] Liluashvili A., Ónody J. and Voigtmann T., *Phys. Rev. E*, **96** (2017) 062608.